

C •

FCTUC FACULDADE DE CIÊNCIAS
E TECNOLOGIA
UNIVERSIDADE DE COIMBRA

Inês Ferreira de Sousa

Development of a magneto-optic device for rapid detection of Malaria

*Dissertation submitted to the University of Coimbra
in fulfilment of the necessary requirements for
obtaining a MSc degree in Biomedical Engineering.*

Under the supervision of
Professor Ph.D. Carlos Correia (GEI, UC)
Eng. Tiago Marçal (GEI, UC)

Coimbra, 2016

This work was developed in collaboration with:



Electronics and Instrumentation Group (GEI)
University of Coimbra, Portugal



Exatronic Insight Innovation
Aveiro, Portugal



Pedro Gomes Design



Matibabu Foundation (MFK)



ResilientAfrica Network (RAN)

Esta cópia da tese é fornecida na condição de que quem a consulta reconhece que os direitos de autor são pertença do autor da tese e que nenhuma citação ou informação obtida a partir dela pode ser publicada sem a referência apropriada.

This copy of the thesis has been supplied on condition that anyone who consults it is understood to recognize that its copyright rests with its author and that no quotation from the thesis and no information derived from it may be published without proper acknowledgement.

Resumo

A malária causou cerca de 214 milhões casos de doença a nível mundial e 238 mil mortes em 2015. Trata-se de uma doença causada por um parasita protozoário conhecido por *Plasmodium* que infeta as células do fígado e os eritrócitos nos humanos. Durante o ciclo intraeritrocitário, o parasita produz hemozoína. As propriedades magnéticas e óticas da hemozoína, bem como a sua dinâmica em fluídos altamente controlada, fazem deste pigmento um potencial alvo para o diagnóstico da malária. O objetivo deste projeto consiste no desenvolvimento de um instrumento magneto-ótico para a deteção rápida da malária, o qual seria útil na prática clínica e na prevenção de resistências aos medicamentos. O dispositivo foi usado para testar diferentes amostras de sangue e uma solução de hemozoína sintética, uma versão artificial da hemozoína.

Foram estudadas as melhores diluições de sangue total para a deteção de um bom sinal, tendo-se verificado que a melhor concentração era a de 1%. O dispositivo foi capaz de detetar a hemozoína sintética, mas é necessário realizar mais testes para validar a sua aplicação no diagnóstico da malária, nomeadamente a sua resposta a sangue infetado, e para determinar a sua sensibilidade.

Palavras-chave: Malária, hemozoína, efeito de Cotton-Mouton, dispositivo magneto-ótico, diagnóstico médico

Abstract

Malaria caused an estimate of 214 million cases worldwide and 438 thousand deaths in 2015. It is a mosquito-borne disease caused by a parasitic protozoan known as *Plasmodium*, which infects human liver cells and erythrocytes. During the intraerythrocytic growth cycle, the parasite produces hemozoin. The magnetic and optical properties of hemozoin as well as its highly controllable dynamics in fluids make this pigment a potential target for the diagnosis of malaria.

The aim of this project is the development of a magneto-optic device for rapid detection of malaria. The creation of a new rapid diagnostic test for malaria would be useful for point-of-care clinics and could prevent the spread of drug resistance. The device was used to test different blood samples and a solution of synthetic hemozoin, an artificial version of hemozoin.

It was studied the best dilutions of whole blood for a good signal detection, being observed that it corresponds to 1% concentration. The device was capable of detecting the synthetic hemozoin, but it is necessary to realize more tests to validate its use on the diagnosis of malaria, namely the response of the device with infected blood, and to determine its sensibility.

Keywords: Malaria, hemozoin, Cotton-Mouton effect, magneto-optic device, medical diagnostics

List of Figures

1.1	Endemic countries [2].	1
1.2	Hemozoin Crystal Structure [10].	4
3.1	Structure of the Halbach cylinder [21].	11
3.2	Original scheme of detection.	12
3.3	MAPS-010-100 [22] (left) and MAPS-F10-100 [23] (right)	13
4.1	Signal detected with different ink concentrations.	18
4.2	Results obtained with sHZ for the upper photodiode. . .	18
4.3	Results obtained with sHZ for the lower photodiode. . .	18
4.4	Signal detected with different concentrations of blood sample 4.	28
4.5	Signal detected with different concentrations of blood sample 13.	29

List of Tables

1.1	Aims of Treatment [7].	3
2.1	Parasitaemia and clinical correlates for <i>P. falciparum</i> [13].	5
3.1	Components of PBS solution.	15
3.2	Volumes used in the preparation of the solutions.	15
4.1	Signal detected with different ink concentrations.	17
4.2	Results obtained with blood samples 1, 2, 3 and 4	20
4.3	Results obtained with blood samples 5, 6, 7 and 8	21
4.4	Results obtained with blood samples 9, 10, 11 and 12	22
4.5	Results obtained with blood samples 13, 14 and 15	23
4.6	Results obtained with blood samples 1, 3, 4 and 5	24
4.7	Results obtained with blood samples 6, 7, 8 and 9	25
4.8	Results obtained with blood samples 10, 11, 2 and 12	26
4.9	Results obtained with blood samples 13 and 14	27
4.10	Signal detected in the lower photodiode for different concentrations of blood sample 4.	28
4.11	Signal detected in the lower photodiode for different concentrations of blood sample 13.	29
1	Blood Samples Data	39
2	Results obtained with blood samples 1 and 2	42

Acronyms

WHO World Health Organization

P. *Plasmodium*

ACT Artemisinin-based Combination Therapy

POC Point-of-care

sHZ Synthetic Hemozoin

RDTs Rapid Diagnostic Tests

HRP-2 Histidine-rich Protein 2

NATs Nucleic Acid Tests

PCR Polymerase Chain Reaction

EIS Electrical Impedance Spectroscopy

PBS Phosphate-buffered Saline

Contents

1	Introduction	1
1.1	Epidemiology and Impact of Malaria	1
1.2	Background	2
1.3	Objective	4
2	State of the Art	5
2.1	Current Diagnostic Methods	5
2.1.1	Giemsa Microscopy	6
2.1.2	Rapid Diagnostic Tests	6
2.1.3	Polimerase Chain Reaction	7
2.2	Methods in Study	7
2.2.1	Nucleic Acid Tests	7
2.2.2	Electrical Impedance Spectroscopy	8
2.2.3	Magneto-Optic Method	8
3	Methods	11
3.1	Description of the Device	11
3.1.1	Characterization of the Cuvettes	12
3.2	Characterization of the Red Ink	13
3.3	Characterization of the synthetic hemozoin	14
3.4	Characterization of Whole Blood	14
3.5	Data processing	15
4	Results	17
4.1	Red Ink Test	17
4.2	Synthetic Hemozoin Test	18

4.3	Whole Blood Tests	19
4.3.1	Additional Tests	28
5	Conclusion	31
5.1	Future Work	32
	Appendices	37

Chapter 1

Introduction

1.1 Epidemiology and Impact of Malaria

Malaria is endemic in 97 countries and territories around the world, putting 3.3 billion people at risk of infection, and is responsible for most of the health costs in low-income countries [1]. The global distribution of malaria in 2014 is highlighted in Figure 1.1.

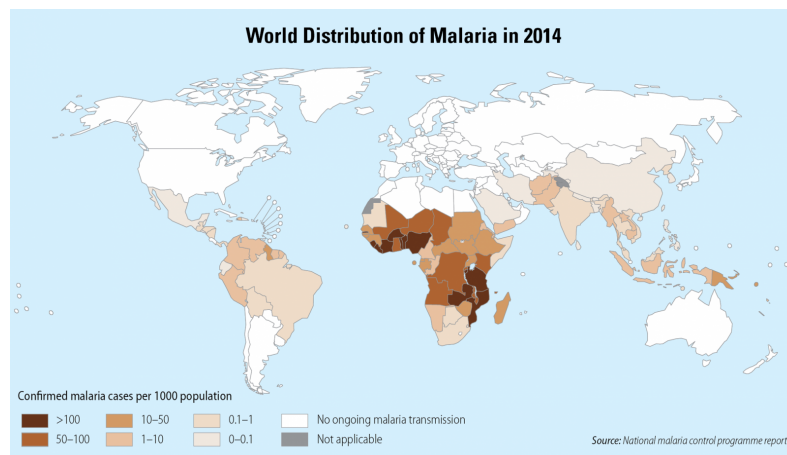


Figure 1.1: Endemic countries [2].

World Health Organization (WHO) reported that in 2015 were estimated 214 million cases of malaria worldwide, and 438 thousand deaths of which 306 thousand were children aged under 5 years [3].

Most of the estimated cases occurred in the WHO African Region (88%),

followed by the WHO South-East Asian Region (10%) and the WHO Eastern Mediterranean Region (2%). Similarly, it is estimated that most deaths (90%) were in the WHO African Region, followed by the WHO South-East Asian Region (7%) and the WHO Eastern Mediterranean Region (2%) [1,3].

Despite the fact that malaria continues to be responsible for the death of many children, there was a remarkable reduction of cases and deaths between 2000 and 2015. It is estimated a reduction of 37% in incidence and 60% in mortality of the disease, in the referred period. The same is observed in children under 5 years between 1990 and 2015 with an estimated decrease in mortality by two thirds [3].

In order to prevent more deaths and reduce transmission it is important an early diagnosis and treatment of the disease. However, the first symptoms of malaria are non specific and similar to those of a minor systemic viral illness which difficult the diagnosis. If treated, a rapid and full recovery is expected. Otherwise, particularly in *Plasmodium falciparum* malaria, the parasite burden continues to increase and the patient may develop potentially lethal severe malaria [4].

The treatment of malaria varies according with the evading parasite. Artemisinin-based combination therapy (ACT) is recommended for the treatment of *P. falciparum* malaria [5]. However, in areas of multiple-drug-resistant *P. falciparum* the use of quinine has been reestablished [6]. In areas of low transmission, the first line for the treatment of *P. vivax* and *P. ovale* is chloroquine, while for the liver stage of *P. vivax* it is used primaquine [5]. More detailed information about the different treatments of malaria is exposed in Table 1.1.

1.2 Background

Malaria is a mosquito-borne disease caused by a parasitic protozoan known as *Plasmodium* (*P.*). The five species of parasites that infect humans are: *P. falciparum*, *P. vivax*, *P. ovale*, *P. malariae* and *P. knowlesi*. Unlike the first four parasites that are spread from one person to another

Table 1.1: Aims of Treatment [7].

Aim	Cause	Drugs
To relieve symptoms	Symptoms are caused by blood forms of the parasite	Chloroquine, quinine, ACT
To prevent relapses	Relapses are due to hypnozoites of <i>P. vivax</i> / <i>P. ovale</i>	Primaquine
To prevent spread	Spread is through the gametocytes	Primaquine for <i>P. falciparum</i> , Chloroquine for all other

via the bite of an infected female *Anopheles* mosquito, the latter is transmitted when the mosquito is infected by a monkey (zoonotic transmission) and is being recently reported in the forested regions of South-East Asia and in the island of Borneo [3, 4, 8].

The parasite development in human hosts comprises two cycles: the exoerythrocytic schizogony, that takes place in the liver; and the intraerythrocytic schizogony, that occurs in the erythrocytes. The blood stage parasites are the ones responsible for the clinical manifestations of the disease [8].

During the intraerythrocytic growth cycle there are structural, mechanical and biochemical alterations in the host erythrocytes. Structural changes include the development of parasitophorous vacuoles and the formation of adherent protrusions on the erythrocytes' membrane. Mechanical modifications comprise the loss of erythrocytes deformability and an increase of adherence of infected erythrocytes to the vascular endothelium or other erythrocytes [9]. The most important biochemical alteration is the digestion of cytosolic hemoglobin proteins (goblin) with the formation of monomeric heme. As heme is highly toxic to the parasite, it is converted into an insoluble crystallized form called hemozoin, where the heme groups are dimerized through iron-carboxylate links and its three dimensional structure is stabilized by hydrogen bonds. Additionally, there is a change in the valency and in the local coordination of iron which promotes the transformation of low-spin Fe^{2+} diamagnetic oxyhemoglobin into high-spin Fe^{3+} paramagnetic hemozoin, which, in

turn, produces an alteration of the magnetic state and susceptibility [9 - 11].

Hemozoin is deposited in vacuoles within the erythrocytes, and then released into suspension in the plasma upon the rupture of infected cells, from where it is ultimately scavenged by leukocytes [12]. The morphology of the crystallites varies with the parasite species, however, they typically have an elongated rod like shape as shown in Figure 1.2. There is an artificially grown version of hemozoin called synthetic hemozoin (sHZ). It was demonstrated that they share identical chemical composition, crystal structure and optical and magnetic properties [10]. The presence of hemozoin in blood or tissue is a positive indicative of malaria infection [12].

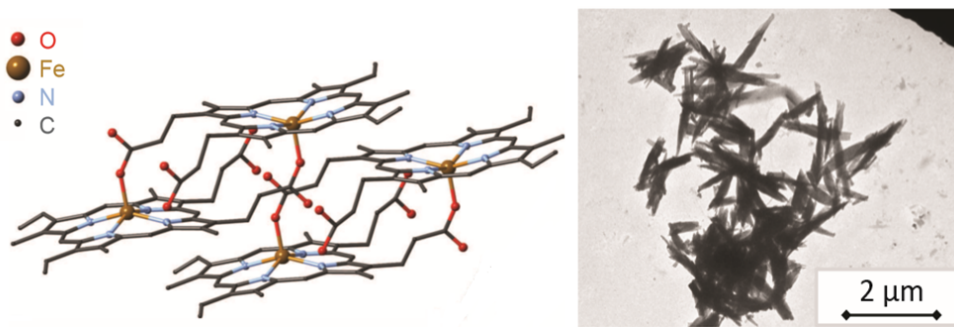


Figure 1.2: Structure and morphology of hemozoin crystals [10].

1.3 Objective

The aim of this project was to study the application of the magneto-optic effect in a portable device for rapid detection of the malaria parasite at point-of-care (POC) clinics. This idea surged from the need to detect the disease at an early stage and to avoid the spread of drug resistance due to the misdiagnosis of patients.

Chapter 2

State of the Art

2.1 Current Diagnostic Methods

The severity of the disease depends on the parasite count [13]. Table 2.1 presents some values of parasitemia and the corresponding clinical findings.

WHO recommends Giemsa microscopy and Rapid Diagnostic Tests (RDTs) to diagnose malaria. However, alternative methods have been studied in order to achieve lower limits of detection and to be applied in the field.

Table 2.1: Parasitaemia and clinical correlates for *P. falciparum* [13].

Parasitaemia (%)	Parasite/ μL	Remarks
0.0001 – 0.0004	5 – 20	Sensitivity of thick blood film
0.002	100	Patients may have symptoms below this level
0.2	10,000	Level above which immune patients exhibit symptoms
2	100,000	Maximum parasitaemia of <i>P. vivax</i> and <i>P. ovale</i>
2 – 5	100,000 – 250,000	Hyperparasitaemia/severe malaria, increased mortality
10	500,000	Transfusion may be considered/high mortality

2.1.1 Giemsa Microscopy

The gold standard for the diagnosis of malaria is Giemsa-stained blood microscopy. This test requires a skilled technician capable of reading the blood smears. There are two different staining techniques: the thin and the thick blood smear. In the thin blood smear, the parasite morphology is preserved more accurately and it is easier to identify the species, while in the thick blood smear it is possible to observe a large volume of blood more quickly, which increases the sensitivity of the diagnosis. However, in the thick blood smear it is more difficult to identify the infecting parasite because of distortions in the morphology [14]. A highly trained technician can reliably detect as few as 10 parasites/ μL of blood [12].

There is a growing consensus that Giemsa-stained blood microscopy is inadequate for malaria diagnosis because the quality of the examination is highly dependent on the quality of the microscope, the quality of the staining reagents used and the skills of the technician, so the highest sensitivities are rarely obtained outside specialised laboratories. In addition this technique is time consuming and subject to significant variability in its application, that depends on the number of fields examined and the methodology employed [11, 14].

2.1.2 Rapid Diagnostic Tests

Nowadays RDTs consist of a small, disposable kits in which a drop of blood from the patient, usually 5 to 15 μL , is mixed with an absorbent chemical strip to detect specific antigens that the parasites produce. This device uses immunochromatographic assay with the monoclonal antibodies, directed against the target parasite antigen, impregnated on the test strip. The principal targets of RDTs are histidine-rich protein 2 (HRP-2) antigens, a protein specific to *P. falciparum*; and parasite lactate dehydrogenase enzymes, that can be species-specific for *P. falciparum* and *P. vivax* or detect all malaria species (pan-specific). A minority uses Plasmodium aldolase as a pan-species target antigen. RDTs can detect one or more of the three target antigens aforementioned. The result, usually a coloured test line, is obtained in 5 to 20 minutes, and the limit of

detection has been reported to be more than 100 parasites/ μL [14, 15]. RDTs typically have a shelf-life of 18 to 24 months and they are easy to use and accurate, which allows their use in most healthcare settings [16]. Additionally, RDTs are more likely to be cost-effective than microscopy. However, there is a wide variability between RDTs that is especially high when parasitemia is less than 200 parasites/ μL of blood. Some of this variability is attributed to the variation in the incidence and structure of the HRP-2 antigen. In addition, RDTs degrade and become less sensitive and specific at temperatures commonly found in POC clinics, and might give false-positive results because HRP-2 antigens can keep circulating in the patient's blood for weeks after successful treatment [14].

2.1.3 Polimerase Chain Reaction

Nested-Polimerase Chain Reaction (PCR) amplification is one of the most commonly used Nucleic Acid Tests (NATs) for parasite detection. As most of the NATs for malaria, PCR targets the 18S ribosomal RNA gene or its associated messenger RNA, which has regions conserved across all *P.* species and regions specific to each specie [14, 16].

PCR is more sensitive than microscopy and RDTs, having a limit of detection of 0.5 to 5 parasites/ μL . However, its application on POC clinics is limited [14].

2.2 Methods in Study

2.2.1 Nucleic Acid Tests

The possible application of NATs, such as loop-mediated isothermal amplification and nucleic acid sequence-based amplification, at POC clinics has been studied. Many NATs have the amplification step separated from the detection step because initially there is insufficient parasite genetic material for direct detection, which increases the sensitivity [14, 16].

NATs are better for the detection of low level infections, and give results that are less subjective than those of microscopy and RDTs [14]. In

addition, these tests are able to identify the infecting parasite, test for drug resistance and, if appropriately calibrated and targeted, some of them can quantify the parasites [16].

2.2.2 Electrical Impedance Spectroscopy

Recently it has been studied the microfluidic Electrical Impedance Spectroscopy (EIS) as a means of rapid diagnosis for malaria. This analytical technique detects the malaria parasite by distinguish the electrical properties of infected erythrocytes from healthy erythrocytes. This is possible because the charge density of the infected erythrocytes surface is altered by the proteins produce by the parasite [17, 18].

The results obtained by research groups show that it is possible to use impedance measurements to distinguish non-infected blood from malaria-infected blood [17]. The microfluidic EIS is a label-free technique that has some advantages over the others, for instance, it can be produced at low cost as a portable device powered by a battery that gives a quantitative result [19].

2.2.3 Magneto-Optic Method

The magneto-optic method uses the unique properties of hemozoin crystals for the rapid diagnosis of malaria [12]. Hemozoin crystals suspended in a liquid are normally randomly oriented. If the suspension is subject to a rotating magnetic field, the crystals experience a torque that orientates them along the direction of that field [10].

The alignment of the crystals is optically manifested as an induced dichroism, and consequently hemozoin starts to behave as a weak polariser similar to a polaroid, when all crystals are fully orientated. Magneto-optically this phenomenon is analogous to the Cotton-Mouton effect [12].

Grimberg et all. developed a device that applies a high and a low magnetic state to the sample. In the high magnetic state, the crystals tend to orientate, in general, perpendicular to the field direction. When the light polarization is collinear with the field direction part of the light

beam is suppressed by the crystals and when it is perpendicular to the field direction there is an increase of light that passes through blood. At low magnetic state a zero-to-near-zero magnetic field is applied and the crystal are randomly oriented. The difference measurement between the high magnetic state and the low magnetic state corresponds to the amount of parasitemia in the blood sample [20].

Chapter 3

Methods

3.1 Description of the Device

In the developed device, the primary power supply is the power distribution grid of 220 V. This device has two supports for the sample. One of them is inserted into a Halbach cylinder that applies a constant magnetic field of $\frac{1}{4}$ T to the sample and cancels the field to near zero outside the cylinder. This cylinder is formed by a display of 12 magnets and is rotated by a stepper motor that is controlled by the software. The structure of the cylinder is represented in Figure 3.1.

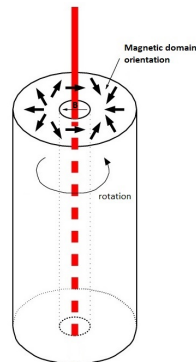


Figure 3.1: Structure of the Halbach cylinder [21].

Inside the Halbach cylinder there are two laser diodes of 650 nm connected to a film polariser, that presents an 80% transmission, and on the opposite side there is a second film polariser display right before the two

photodiodes. While in the upper photodiode the film polariser has its optical axis rotated 90° relatively to the first polariser, in the lower photodiode they are parallel to each other. The gain of the photodiodes was adjusted in order to obtain a higher signal with the upper photodiode and decrease the signal in the lower photodiode. The scheme of detection is represented in Figure 3.2.

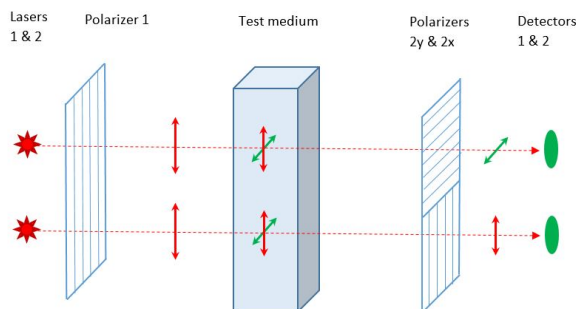


Figure 3.2: Original scheme of detection.

The optical beam is linearly polarised after passing through the first film polariser and when passing through the sample it is expected that two states of polarization arise as a result of the optical dichroism of the hemozoin crystals. This is accomplished by rotating the Halbach cylinder that makes the magnetic field vary between states aligned along and orthogonal to the optical beam. The hemozoin concentration can be determined by calculating the ratio between the states parallel and orthogonal that are detected in the lower and upper photodiode, respectively.

The device was controlled using a Matlab Graphical User Interface, and it was used the waveforms SDK to allow data exchange with Digilent Analog Discovery Hardware.

3.1.1 Characterization of the Cuvettes

During the initial experiences, it was noticed that the cuvettes available, MAPS-F10-100 (fluorometer cuvette) and MAPS-010-100 (spectrophotometer cuvette), had an effect over the plane of polarization of the optical beam. Figure 3.3 represents the cuvettes tested.



Figure 3.3: MAPS-010-100 [22] (left) and MAPS-F10-100 [23] (right)

As expected in a free medium, with no obstacles, the signal detected in the upper photodiode is null. This can be explained by the fact that the light that passes through the first polariser has a different plane of polarization from the second polariser, resulting in the blockage of all the light in the latter. However, when the process was repeated with an empty cuvette, it was registered an increased amplitude, which lead us to conclude that the scattering in the cuvette changes the plane of polarization. Although both cuvettes were made of polystyrene, MAPS-010-100 introduce less dispersion.

In light of these discoveries, it was used MAPS-010-100 in the following tests and the scheme of detection was changed. In the new scheme, it was remove the second film polariser and the concentration of hemozoin corresponds to the difference between the signal detected when the optical beam is parallel and orthogonal to the magnetic field direction.

3.2 Characterization of the Red Ink

The red ink used was from Sheaffer and this colour was chosen because of the lasers wavelength. This colour absorbs less light than the others, and it is the one that resembles more the blood colour. For the ink dilutions it was used distilled (bi-demineralized) water.

3.3 Characterization of the synthetic hemozoin

The sHZ solution was borrowed from the Institute of Molecular Medicine localized in Santa Maria Hospital in Lisbon. The sample was synthesised in the Institute and had a 1mg/mL concentration.

3.4 Characterization of Whole Blood

There were studied blood samples provided by the National Institute of Legal Medicine and Forensic Sciences in Coimbra. In total there were tested 15 blood samples, 7 from Madeira Island and 8 from the Continent. The blood samples, with the exception of the sample 13, were accommodated in a tube with potassium fluoride and Na₂ EDTA, anti-coagulants and preservatives for blood. Blood sample 13 was collected from the cardiac region of a cadaver, and selected to be tested due to the detection of quinine in it. Blood samples 13 to 15 were collected over the last month, so they were fresh at the time of the analysis, unlike the other 12 samples that were collected over the last years.

The blood was not tested for malaria prior to the analysis and the information available is presented in Appendix A. Accordingly to the literature, erythrocytes cause strong light scattering over the visible range, so all blood samples used were hemolyzed, slightly reducing this phenomenon. In order to improve the signal read in the photodiodes, the blood was diluted with phosphate-buffered saline (PBS) solution (pH 7), prepared in the Institute. The components of the buffer solution are described in Table 3.1. To fill each cuvette it was necessary a volume of 4 mL. The volumes used to prepare these solutions are discriminated in Table 3.2.

Table 3.1: Components of PBS solution.

Solution components/mobile phase	Internal Code	Quantity
Potassium Chloride	RG470MK003	400 mg
Sodium Chloride	RG469MK007	16 g
Potassium Dihydrogenophosphate	RG473MK020	400 mg
Disodium Hydrogenophosphate	RG474MK010	2,3 g
8.5% Phosphoric Acid	SR714MK010	Drops
Water	-	until 2L

Table 3.2: Volumes used in the preparation of the solutions.

Concentration	PBS volume (mL)	Whole Blood volume (μ L)
1%	4,95	50
2%	4,90	100
4%	4,80	200
6%	4,70	300
8%	4,60	400
10%	4,50	500
20%	4,00	1000
50%	2,00	2000

3.5 Data processing

Each acquisition made by the device origins a .txt document with 16 measures. For the tests with red ink and blood samples 4 and 13, it was used the lower photodiode during the acquisitions. The measures were obtained for different concentrations and the tests were repeated three times. Then it was calculated the average and standard deviation of the results.

The graphics of the blood samples and sHZ were obtained by using a script in Matlab, that calculated the average amplitude measured while the Halbach cylinder rotated 360° . Each point in the graphic gives the averaged amplitude of the signal for 15° rotation of the Halbach cylinder. It was chosen a time of 5 seconds between acquisitions to allow the orientation of the sHZ crystals.

Chapter 4

Results

4.1 Red Ink Test

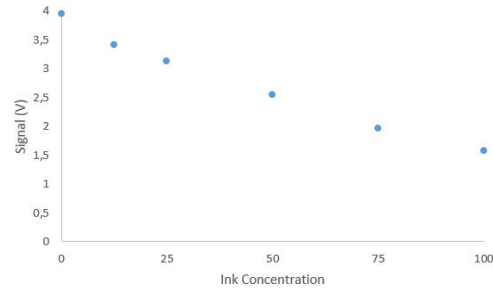
There were used concentrations of 0%, 12.5%, 25%, 50%, 75% and 100%. The acquisitions were made by the lower photodiode, because the upper photodiode saturated. The results obtained are presented in Table 4.1 and the graphic is displayed in Figure 4.1.

Table 4.1: Signal detected with different ink concentrations.

Ink Concentration (%)	Signal (V)	Uncertainty ($\times 10^{-3} \Delta V$)
0	3,957	5,728
12,5	3,415	8,740
25	3,129	8,467
50	2,550	3,001
75	1,972	1,225
100	1,581	2,309

By observation of the Figure 4.1 it is clear that the signal measured by the device is linear with the concentration of ink in the solution. The signal detected has a good amplitude for the range of concentrations studied and the error bars are too small to be noticed, because the measures obtained in the same conditions are very close.

Figure 4.1: Signal detected with different ink concentrations.



4.2 Synthetic Hemozoin Test

It was studied the behaviour of the sHZ solution submitted to a rotational magnetic field of 360° . The results are presented in Figures 4.2 and 4.3.

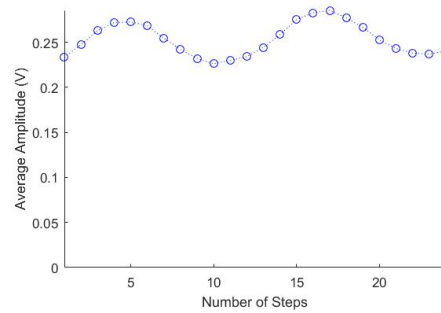


Figure 4.2: Results obtained with sHZ for the upper photodiode.

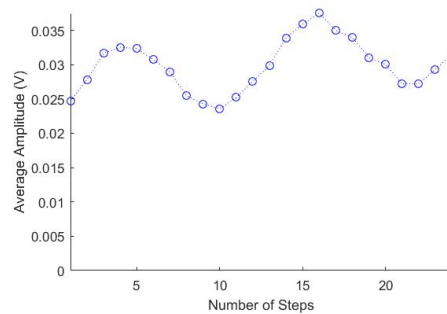


Figure 4.3: Results obtained with sHZ for the lower photodiode.

These figures show the relation between the signal measured in the photodiodes and the angular variation of the magnetic field while an optical beam passes through the sample. The hemozoin crystals align along the

field applied and follow its movement. Due to the rod like shape of the crystals, when they are aligned along the optical beam more light can pass through the sample than when they are aligned orthogonally. As a result, it is obtained a modulated signal. Accordingly with these results, it is proved that the sHz crystals respond to and align with the field applied.

4.3 Whole Blood Tests

There were used different concentrations of whole blood diluted in PBS to analyse the response of both photodiodes. For the lower photodiode it was necessary to dilute more the whole blood, while the upper photodiode was able to detect the laser light in more turbid samples.

Initially it was tested blood sample 1 for concentrations of 100%, 50%, 10%, 5% and 1%. For the lower photodiode, the signal was null for 100% and 50% concentrations, saturated for 10% concentration and had a good amplitude for the lower concentrations. For the upper photodiode, the signal was very low for 100% and 50% concentrations and saturated with 1% and 5% concentrations, having only a good amplitude for 10% concentration.

Blood samples 2 and 3 were tested for concentrations of 50%, 10%, 5% and 1%. With blood sample 2 the upper photodiode detected a higher signal for 50% concentration and saturated for 10% concentration.

The graphics obtained with blood sample 1, for 100% and 50% concentrations, and with blood sample 2, for 50% concentration, are displayed in Appendix B.

Taking that into account it was chosen a concentration of 10% and 1% for the study of the remaining samples.

Due to the low volume available of blood sample 15 it was only analysed a concentration of 1%.

Tables 4.2, 4.3, 4.4 and 4.5 display the graphics obtained with 1% concentration and Tables 4.6, 4.7, 4.8 and 4.9 present the graphics for 10% concentration.

Table 4.2: Results obtained with blood samples 1, 2, 3 and 4

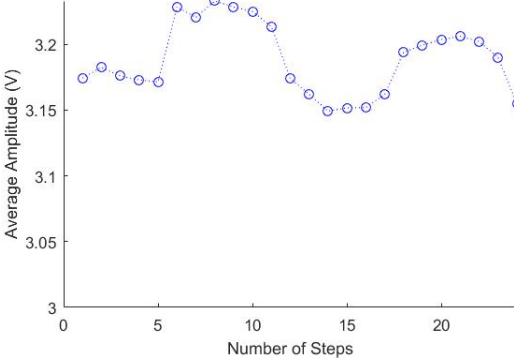
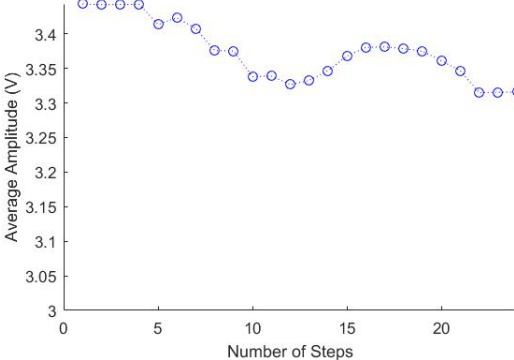
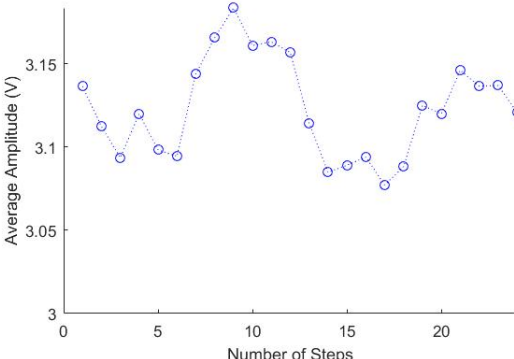
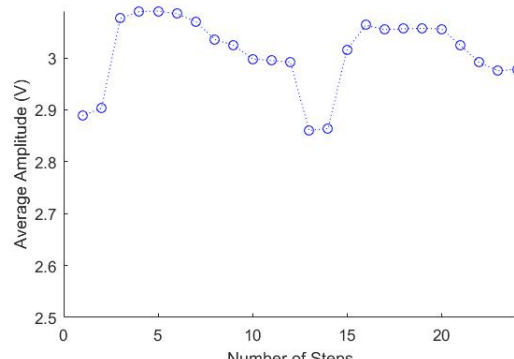
Sample	Lower Photodiode 1%
1	 <p>Average Amplitude (V)</p> <p>Number of Steps</p>
2	 <p>Average Amplitude (V)</p> <p>Number of Steps</p>
3	 <p>Average Amplitude (V)</p> <p>Number of Steps</p>
4	 <p>Average Amplitude (V)</p> <p>Number of Steps</p>

Table 4.3: Results obtained with blood samples 5, 6, 7 and 8

Sample	Lower Photodiode 1%
5	<p>Average Amplitude (V)</p> <p>Number of Steps</p>
6	<p>Average Amplitude (V)</p> <p>Number of Steps</p>
7	<p>Average Amplitude (V)</p> <p>Number of Steps</p>
8	<p>Average Amplitude (V)</p> <p>Number of Steps</p>

Table 4.4: Results obtained with blood samples 9, 10, 11 and 12

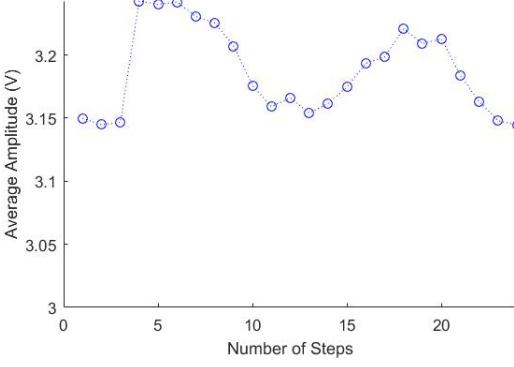
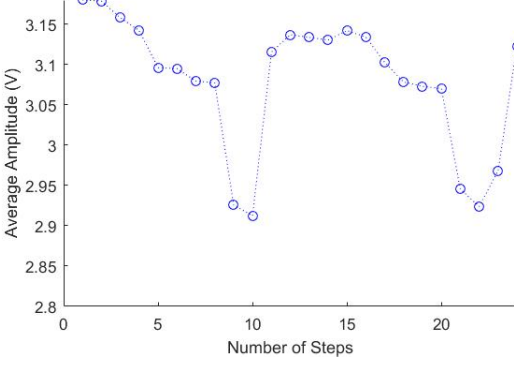
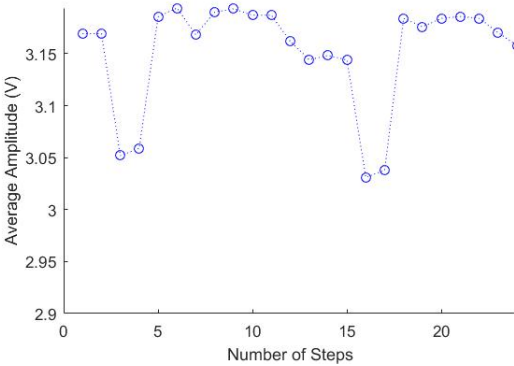
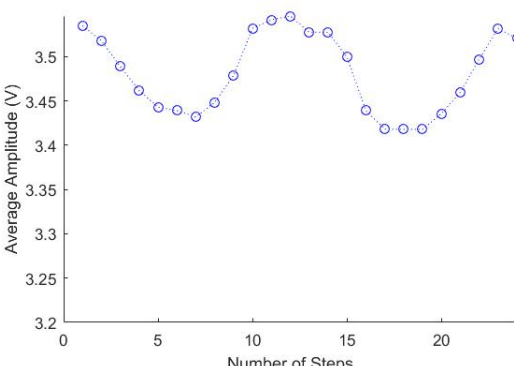
Sample	Lower Photodiode 1%
9	 <p>Average Amplitude (V) vs Number of Steps for Sample 9. The graph shows a fluctuating trend with a peak of approximately 3.25 V at 5 steps and another peak of approximately 3.25 V at 18 steps.</p>
10	 <p>Average Amplitude (V) vs Number of Steps for Sample 10. The graph shows a significant dip to approximately 2.92 V at 10 steps and another dip to approximately 2.93 V at 22 steps.</p>
11	 <p>Average Amplitude (V) vs Number of Steps for Sample 11. The graph shows a dip to approximately 3.05 V at 3 steps and another dip to approximately 3.03 V at 16 steps.</p>
12	 <p>Average Amplitude (V) vs Number of Steps for Sample 12. The graph shows a dip to approximately 3.45 V at 5 steps and another dip to approximately 3.43 V at 17 steps.</p>

Table 4.5: Results obtained with blood samples 13, 14 and 15

Sample	Lower Photodiode 1%																																																		
13	<table border="1"> <caption>Data for Sample 13</caption> <thead> <tr> <th>Number of Steps</th> <th>Average Amplitude (V)</th> </tr> </thead> <tbody> <tr><td>1</td><td>3.45</td></tr> <tr><td>2</td><td>3.43</td></tr> <tr><td>3</td><td>3.42</td></tr> <tr><td>4</td><td>3.41</td></tr> <tr><td>5</td><td>3.37</td></tr> <tr><td>6</td><td>3.35</td></tr> <tr><td>7</td><td>3.34</td></tr> <tr><td>8</td><td>3.33</td></tr> <tr><td>9</td><td>3.34</td></tr> <tr><td>10</td><td>3.34</td></tr> <tr><td>11</td><td>3.34</td></tr> <tr><td>12</td><td>3.38</td></tr> <tr><td>13</td><td>3.39</td></tr> <tr><td>14</td><td>3.39</td></tr> <tr><td>15</td><td>3.40</td></tr> <tr><td>16</td><td>3.38</td></tr> <tr><td>17</td><td>3.36</td></tr> <tr><td>18</td><td>3.34</td></tr> <tr><td>19</td><td>3.34</td></tr> <tr><td>20</td><td>3.34</td></tr> <tr><td>21</td><td>3.34</td></tr> <tr><td>22</td><td>3.20</td></tr> <tr><td>23</td><td>3.20</td></tr> <tr><td>24</td><td>3.39</td></tr> </tbody> </table>	Number of Steps	Average Amplitude (V)	1	3.45	2	3.43	3	3.42	4	3.41	5	3.37	6	3.35	7	3.34	8	3.33	9	3.34	10	3.34	11	3.34	12	3.38	13	3.39	14	3.39	15	3.40	16	3.38	17	3.36	18	3.34	19	3.34	20	3.34	21	3.34	22	3.20	23	3.20	24	3.39
	Number of Steps	Average Amplitude (V)																																																	
	1	3.45																																																	
2	3.43																																																		
3	3.42																																																		
4	3.41																																																		
5	3.37																																																		
6	3.35																																																		
7	3.34																																																		
8	3.33																																																		
9	3.34																																																		
10	3.34																																																		
11	3.34																																																		
12	3.38																																																		
13	3.39																																																		
14	3.39																																																		
15	3.40																																																		
16	3.38																																																		
17	3.36																																																		
18	3.34																																																		
19	3.34																																																		
20	3.34																																																		
21	3.34																																																		
22	3.20																																																		
23	3.20																																																		
24	3.39																																																		
14	<table border="1"> <caption>Data for Sample 14</caption> <thead> <tr> <th>Number of Steps</th> <th>Average Amplitude (V)</th> </tr> </thead> <tbody> <tr><td>1</td><td>3.43</td></tr> <tr><td>2</td><td>3.43</td></tr> <tr><td>3</td><td>3.45</td></tr> <tr><td>4</td><td>3.63</td></tr> <tr><td>5</td><td>3.65</td></tr> <tr><td>6</td><td>3.65</td></tr> <tr><td>7</td><td>3.65</td></tr> <tr><td>8</td><td>3.65</td></tr> <tr><td>9</td><td>3.64</td></tr> <tr><td>10</td><td>3.58</td></tr> <tr><td>11</td><td>3.56</td></tr> <tr><td>12</td><td>3.56</td></tr> <tr><td>13</td><td>3.56</td></tr> <tr><td>14</td><td>3.43</td></tr> <tr><td>15</td><td>3.43</td></tr> <tr><td>16</td><td>3.60</td></tr> <tr><td>17</td><td>3.63</td></tr> <tr><td>18</td><td>3.63</td></tr> <tr><td>19</td><td>3.63</td></tr> <tr><td>20</td><td>3.63</td></tr> <tr><td>21</td><td>3.62</td></tr> <tr><td>22</td><td>3.61</td></tr> <tr><td>23</td><td>3.56</td></tr> </tbody> </table>	Number of Steps	Average Amplitude (V)	1	3.43	2	3.43	3	3.45	4	3.63	5	3.65	6	3.65	7	3.65	8	3.65	9	3.64	10	3.58	11	3.56	12	3.56	13	3.56	14	3.43	15	3.43	16	3.60	17	3.63	18	3.63	19	3.63	20	3.63	21	3.62	22	3.61	23	3.56		
Number of Steps	Average Amplitude (V)																																																		
1	3.43																																																		
2	3.43																																																		
3	3.45																																																		
4	3.63																																																		
5	3.65																																																		
6	3.65																																																		
7	3.65																																																		
8	3.65																																																		
9	3.64																																																		
10	3.58																																																		
11	3.56																																																		
12	3.56																																																		
13	3.56																																																		
14	3.43																																																		
15	3.43																																																		
16	3.60																																																		
17	3.63																																																		
18	3.63																																																		
19	3.63																																																		
20	3.63																																																		
21	3.62																																																		
22	3.61																																																		
23	3.56																																																		
15	<table border="1"> <caption>Data for Sample 15</caption> <thead> <tr> <th>Number of Steps</th> <th>Average Amplitude (V)</th> </tr> </thead> <tbody> <tr><td>1</td><td>3.75</td></tr> <tr><td>2</td><td>3.76</td></tr> <tr><td>3</td><td>3.74</td></tr> <tr><td>4</td><td>3.74</td></tr> <tr><td>5</td><td>3.75</td></tr> <tr><td>6</td><td>3.78</td></tr> <tr><td>7</td><td>3.79</td></tr> <tr><td>8</td><td>3.80</td></tr> <tr><td>9</td><td>3.81</td></tr> <tr><td>10</td><td>3.80</td></tr> <tr><td>11</td><td>3.78</td></tr> <tr><td>12</td><td>3.75</td></tr> <tr><td>13</td><td>3.74</td></tr> <tr><td>14</td><td>3.73</td></tr> <tr><td>15</td><td>3.73</td></tr> <tr><td>16</td><td>3.73</td></tr> <tr><td>17</td><td>3.77</td></tr> <tr><td>18</td><td>3.79</td></tr> <tr><td>19</td><td>3.81</td></tr> <tr><td>20</td><td>3.82</td></tr> <tr><td>21</td><td>3.82</td></tr> <tr><td>22</td><td>3.81</td></tr> <tr><td>23</td><td>3.75</td></tr> </tbody> </table>	Number of Steps	Average Amplitude (V)	1	3.75	2	3.76	3	3.74	4	3.74	5	3.75	6	3.78	7	3.79	8	3.80	9	3.81	10	3.80	11	3.78	12	3.75	13	3.74	14	3.73	15	3.73	16	3.73	17	3.77	18	3.79	19	3.81	20	3.82	21	3.82	22	3.81	23	3.75		
Number of Steps	Average Amplitude (V)																																																		
1	3.75																																																		
2	3.76																																																		
3	3.74																																																		
4	3.74																																																		
5	3.75																																																		
6	3.78																																																		
7	3.79																																																		
8	3.80																																																		
9	3.81																																																		
10	3.80																																																		
11	3.78																																																		
12	3.75																																																		
13	3.74																																																		
14	3.73																																																		
15	3.73																																																		
16	3.73																																																		
17	3.77																																																		
18	3.79																																																		
19	3.81																																																		
20	3.82																																																		
21	3.82																																																		
22	3.81																																																		
23	3.75																																																		

Table 4.6: Results obtained with blood samples 1, 3, 4 and 5

Sample	Upper Photodiode 10%
1	<p>Average Amplitude (V)</p> <p>Number of Steps</p>
	<p>Average Amplitude (V)</p> <p>Number of Steps</p>
3	<p>Average Amplitude (V)</p> <p>Number of Steps</p>
4	<p>Average Amplitude (V)</p> <p>Number of Steps</p>
5	

Table 4.7: Results obtained with blood samples 6, 7, 8 and 9

Sample	Upper Photodiode 10%
6	
7	
8	
9	

Table 4.8: Results obtained with blood samples 10, 11, 2 and 12

Sample	Upper Photodiode 10%
10	
11	Lower Photodiode 10%
2	
12	

Table 4.9: Results obtained with blood samples 13 and 14

Sample	Lower Photodiode 10%
13	<p>The graph for Sample 13 shows the average amplitude in Volts (V) on the y-axis (ranging from 1.0 to 1.35) against the number of steps on the x-axis (ranging from 0 to 20). The data points are connected by a dotted line. The amplitude starts at ~1.33V at step 1, dips to ~1.29V at step 4, rises to ~1.34V at step 8, dips to ~1.26V at step 15, and ends at ~1.32V at step 20.</p>
14	<p>The graph for Sample 14 shows the average amplitude in Volts (V) on the y-axis (ranging from 2.02 to 2.12) against the number of steps on the x-axis (ranging from 0 to 20). The data points are connected by a dotted line. The amplitude starts at ~2.11V at step 1, dips to ~2.09V at step 4, rises to ~2.12V at step 8, dips to ~2.06V at step 15, and ends at ~2.07V at step 20.</p>

With 1% concentration, the signals detected with the different blood samples are periodic and have an amplitude that does not vary much between them and, in general, is higher for the fresh blood samples. Blood sample 13 registered a lower signal than the other fresh blood samples, which might be related to the origin of the blood (cadaver). Blood samples 2 and 12 had a higher signal than the recorded for samples 1 to 13, which can be explained by the fact that sample 12 was coagulated, so the actual volume of blood present in solution could be less than thought, while sample 2 was more fluid than the others.

With 10% concentration, the amplitude of the signals measured varies with each sample. For this concentration, the characteristics of the sample, such as colour and viscosity, are more preserved, having a stronger effect on the value measured.

The graphics obtained with blood samples 4, 6, 7, 10, 11, 13 and 14 for 1% concentration and with blood samples 12 and 13 for 10% concentration have a regular behaviour with some points breaking out of the regularity. This can be a result of the conditions of the materials used, particularly the cuvettes. Some of the cuvettes did not had a smooth surface, presenting some risks that might have dispersed the optical beam, and consequently caused some of the irregularities observed.

4.3.1 Additional Tests

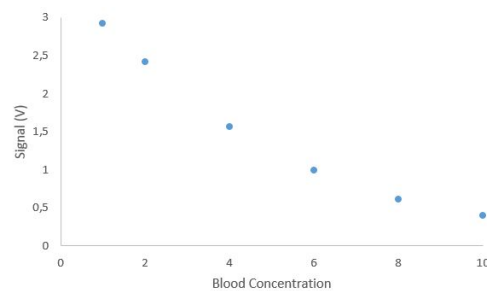
There were used blood samples 4 and 13 to study the variation of the signal detected with the concentration of blood in solution.

For blood sample 4 there were used concentrations of 1%, 2%, 4%, 6%, 8% and 10%. The results obtained are presented in Table 4.10 and the graphic is displayed in Figure 4.4.

Table 4.10: Signal detected in the lower photodiode for different concentrations of blood sample 4.

Blood Concentration (%)	Signal (V)	Uncertainty ($\times 10^{-3} \Delta V$)
1	2,916667	0,002898
2	2,415250	0,002462
4	1,5646604	0,002161
6	0,992771	0,003328
8	0,611625	0,001511
10	0,403250	0,004706

Figure 4.4: Signal detected with different concentrations of blood sample 4.

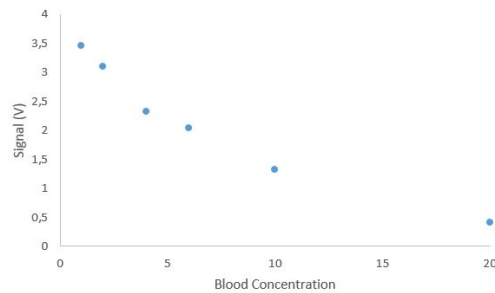


For blood sample 13 it was used concentrations of 1%, 4%, 6%, 10% and 20%. The results obtained are presented in Table 4.11 and the graphic is displayed in Figure 4.5.

Table 4.11: Signal detected in the lower photodiode for different concentrations of blood sample 13.

Blood Concentration (%)	Signal (V)	Uncertainty ($\times 10^{-3} \Delta V$)
1	3,457	2,642
4	2,322	8,819
6	2,039	2,630
10	1,326	8,717
20	0,411	2,228

Figure 4.5: Signal detected with different concentrations of blood sample 13.



With blood samples it was necessary to use higher dilutions than with the red ink, this can be a result of the blood colour, that is a darker red, and its viscosity.

The variation between the signal detected with different concentrations of whole blood in the range of 0 to 10% is more accentuated in blood sample 4. This can be clearly seen by observation of Figure 4.4 where the signal decreases to half of its value when the concentration is quadruplicated. Blood sample 13 registered a higher signal than blood sample 4, this was expected taking it account the results of the previous section. With this sample it was necessary to use higher concentrations of whole blood (20%) to get a measure lower than 1 V. The error bars are to small to be noticed in both graphics.

Chapter 5

Conclusion

By the analysis of the results obtained with the red ink and blood samples 4 and 13, focusing on the values of the standard deviation, it can be said that the device has a good precision.

Considering the results obtained with the blood samples, the concentrations that were found ideal to obtain a good amplitude of signal with both photodiodes were those below 20%, which correspond to a volume of 1 mL of whole blood. Taking into account that this device is to be applied in POC clinics as a means of screening for the malaria parasite, this volume seems to be acceptable. However, if it is to be applied as a routine diagnostic technique, where it is necessary to perform other analysis that typically use 20 to 50 μL of blood per exam, it would be recommended the use of the lowest concentrations. For instance, the 1% concentration, which corresponds to a 50 μL of whole blood in a volume of 5 ml solution, is acceptable in the current practice.

The colour of the blood samples has a strong influence in the amplitude of the signal measured, and that is dependent on the elements present in it. Commonly the samples are dark red, but, for instance, if carbon monoxide or some medications are present, blood is more bright and as a consequence the signal measured is higher. In either cases, it is necessary to dilute the blood sample in order to allow that enough light passes through it and reaches the photodiodes.

The results obtained with fresh blood samples, especially 14 and 15, are

quite important as this device is to be used with blood collected at POC clinics. We can conclude that the signal detected with these samples is not only higher but also more regular. Some of the other blood samples, for example sample 4 and 7, have a signal similar to blood sample 14. This could be a result of a better accommodation of these samples or a more recent time of collection. The best results for all blood samples were obtained with the lower photodiode for 1% concentration of whole blood.

The test with sHZ showed that the crystals respond to the magnetic field.

5.1 Future Work

The following steps pass through the redesign of the prototype in order to facilitate the positioning of the samples between the lasers and the photodiodes. To improve the detection it is necessary to apply a stronger magnetic field capable of aligning all the hemozoin crystals along its direction. In literature the value used is 1 T, so it has to be used stronger magnets to achieve such value.

To test if this device is capable of detecting low concentrations of hemozoin in blood it has to be analysed blood samples infected with malaria. As it is difficult to get these samples in Portugal, one way to test this is to use sHZ crystals suspended in blood. Additionally, to determine the hemozoin concentration and test the limits of detection of the device, it has to be analysed the Cotton-Mouton effect.

Bibliography

- [1] United Nations. The Millenium Development Goals Report. 2015.
- [2] Endemic Countries - Roll Back Malaria
URL <http://www.rollbackmalaria.org/countries/endemic-countries-1>
Accessed: 22 February 2016
- [3] World Health Organization. World Malaria Report 2015. 2015.
- [4] World Health Organization. Treatment of Severe Malaria. *Guidelines For The Treatment of Malaria*. 71-88. 2015
- [5] Malaria Consortium - Artemisinin-based Combination Therapy (ACT) (Pages)
- [6] WHO Model Prescribing Information: Drugs Used in Parasitic Diseases - Second Edition: Protozoa: Malaria: Quinine
URL <http://apps.who.int/medicinedocs/en/d/Jh2922e/2.5.2.html#Jh2922e.2.5.2> Accessed: 17 August 2016
- [7] Treatment of Malaria Malaria Site
URL <http://www.malariasite.com/treatment-of-malaria/#treat-severe-malaria> Accessed: 26 August 2016
- [8] Prevention, CDC - Centers for Disease Control and Prevention. CDC - Malaria - About Malaria - Biology Accessed: 19 February 2016
- [9] Sangyeon Cho, Soomin Kim, Youngchan Kim, and Yongkeun Park. Optical imaging techniques for the study of malaria. *Trends in Biotechnology*, 30(2):7179, 2012.
- [10] A Butykai, A Orbán, V Kocsis, D Szaller, S Bordács, E Tátrai-Szekeres, L F Kiss, A Bóta, B G Vértessy, T Zelles, and I Kézsmárki. Malaria pigment crystals as magnetic micro-rotors: key for high-sensitivity diagnosis. *Scientific reports*, 3:1431, 2013.

- [11] Dave M. Newman, Raphaël J. Matelon, M. Lesley Wears, and Luke B. Savage. The in vivo diagnosis of malaria: Feasibility study into a magneto-optic fingertip probe. *IEEE Journal on Selected Topics in Quantum Electronics*, 16(3):573580, 2010.
- [12] Dave M. Newman, John Heptinstall, Raphaël J. Matelon, Luke Savage, M. Lesley Wears, Jamie Beddow, Martin Cox, Henk D F H Schallig, Petra F Mens. A magneto-optic route toward the in vivo diagnosis of malaria: preliminary results and preclinical trial data. *Biophysical journal*, 95(2):994-1000 2008.
- [13] T. Hnscheid. Diagnosis of malaria: A review of alternatives to conventional microscopy. *Clinical and Laboratory Haematology*, 21(4): 235-245 1999.
- [14] Michael S Cordray, Rebecca R Richards-Kortum. Review : Emerging Nucleic Acid Based Tests for Point-of-Care Detection of Malaria. 87(2):223-230 2012.
- [15] Chansuda Wongsrichanalai, Mazie J Barcus, Sinuon Muth, Awaludin Sutamihardja, Walther H Wernsdorfer. A Review of Malaria Diagnostic Tools : Microscopy and Rapid Diagnostic Test (RDT). 77(2):119-127 2007.
- [16] M L Mcmorrow, M Aidoo, S P Kachur. Malaria rapid diagnostic tests in elimination settings can they find the last parasite?. *Clinical Microbiology and Infection*, 17(11):1624-1631 2011.
- [17] Simão Nunes Paula. Exploring impedance spectroscopy as a mean of malaria diagnostic. November 2014.
- [18] Sungjae Ha, Monica Diez-Silva, E Du, Sung Jae Kim, Jongyoon Han, Ming Dao, Anantha P. Chandrakasan. Microfluidic Electric Impedance Spectroscopy for Malaria Diagnosis. *MicroTAS2012*, 1960-1962 2012.
- [19] Sungjae Ha. A Malaria System Based on Electric Impedance Spectroscopy. May 2011.
- [20] Grimberg, B., Deissler, R., Condit, W., Brown, R., Jones, J. and Bihary, R. (2015). Diagnostic Devices and Methods. US 2015/0377857 A1.
- [21] H. Grote. On the possibility of vacuum QED measurements with gravitational wave detectors. *Physical Review D*, 91(2):022002 2015.

[22] Labbox

URL <https://www.labbox.com/en/products/F0E00/xE30/MAPS/>

Accessed: 6 September 2016

[23] Labbox

URL <https://www.labbox.com/en/products/F0E00/xE30/MAPF/>

Accessed: 6 September 2016

Appendices

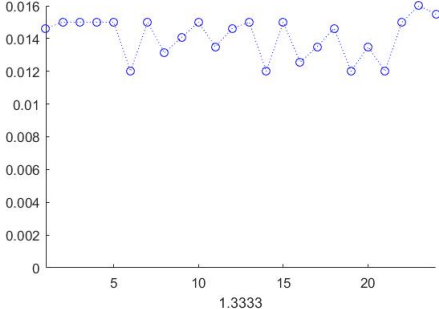
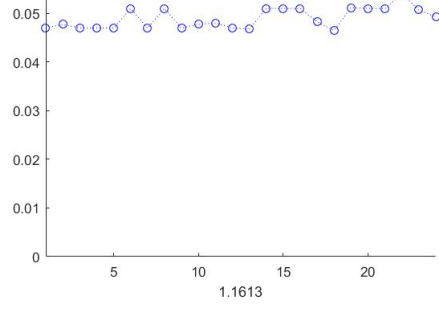
Appendix A

Table 1: Blood Samples Data

Samples	Origin	Age	Sex
#1	Madeira	56	Female
#2	Madeira	39	Male
#3	Madeira	51	Female
#4	Madeira	59	Male
#5	Madeira	64	Female
#6	Madeira	27	Male
#7	Continent - Central Area	20	Male
#8	Continent - Central Area	84	Female
#9	Continent - Central Area	65	Male
#10	Continent - Central Area	61	Male
#11	Continent - Central Area	79	Male
#12	Continent - Central Area	71	Male
#13	Madeira	42	Male
#14	Continent - Central Area	62	Male
#15	Continent - Central Area	52	Female

Appendix B

Table 2: Results obtained with blood samples 1 and 2

Sample	Upper Photodiode 10%
1	
	
Sample	Upper Photodiode 1%
1	